NEAR-CRACK TIP FINITE STRAIN ANALYSIS

P.C.M. Gortemaker, C. de Pater, R.M.E.J. Spiering

Twente University of Technology, Mech. Eng. Dept.
P.O. Box 217, 7500 AE ENSCHEDE, The Netherlands

ABSTRACT

Paper describes numerical work, which has been done on a plane crack problem. A finite element program has been developed for plane stress, plane strain and axisymmetric problems, taking into account geometrical and physical nonlinearity. The frame of reference is a Cartesian resp. cylindrical updated Lagrangian one. The tangent stiffness method applied, comprises constitutive equations relating the Jaumann rate of Cauchy stress to the rate of deformation. The von Mises' yield criterion and the rule of normality has been used. Isotropic and kinematic hardening of the material can be taken into account. The element is the 4-nodes isoparametric quadrilateral one. A modified strain increment has been used to prevent unduly constraints on the modes of deformation. The incremental tangent stiffness solutions are corrected by a subincremental integration and a corrective nodal load technique.
Distribution of true stresses and finite strains at the tip of a plane crack and crack tip opening displacements are obtained for a cyclically loaded cracked tension specimen from elastic-ideally plastic material resp. from AISI-304.

KEYWORDS

Finite element analysis; finite deformations; elastic-plastic stresses; CTOD.

INTRODUCTION

Much attention has been paid to the distribution of stresses and strains around the tips of cracks in linear elastic and elastic-plastic materials. Only a very limited number of these studies however comprise the effects of finite deformations at the crack tip. Rice and Johnson [1] studied this effect in a Prandtl slip line field solution around smoothly blunting cracks. McMeeking [2] performed finite element calculations of cracks taking into account geometrical and physical nonlinearities for power law hardening materials under monotonous loading.
In this contribution finite element results are presented for a cyclically loaded CTS of elasic-ideally plastic material resp. stainless steel type AISI-304.

FUNDAMENTALS

Several papers have been published about the fundamentals of elastic-plastic

finite element analysis, taking into account large deformations. No attempt will be made to give a survey of the field. The reader is therefore referred to the excellent review of Rice et al. [3]. Just the following remarks are being made.
In problems where one has to take into account geometric and/or material non-linearity the solution process is usually a step by step one, where successive increments of prescribed loads and/or displacements are applied in a proportional way.
As a basic feature of a geometric nonlinear problem is that the equilibrium equations must be referred to the deformed geometry, the finite element mesh- fixed relative to material points- has to convect with the deformations.
In the "updated Lagrangian" formulation that has been used, the mesh is updated during the solution process.
Thus by applying the load in increments one may properly take into account the spread of plasticity and the change in geometry of the structure.
The equations governing the problem are most conveniently written down in the form of rate equations related to a current deformed configuration at time t.
The assumption is made that in this configuration all the variables as nodal point coordinates, stresses, strains and stress history are known. The stresses and prescribed surface forces (neglecting body forces) satisfy the equilibrium conditions (in the finite element sense) and the displacement field is continuous and satisfies prescribed displacements at the boundaries. Bases of the finite element formulation are the virtual power equation, describing instantaneous static equilibrium and the material rate of virtual power equation, describing continuing equilibrium of the quasi-static process of deformation. Both these equations must be satisfied at any time during the deformation process for velocities restricted to the set of continuous, piecewise differentiable functions containing the nodal velocities as parameters.
The virtual power equation neglecting volume forces in the current configuration and referred to this configuration is

$$\int_V \sigma_{ij}\delta d_{ij} dV = \int_{S_T} T_i \delta v_i dS_T \qquad (1)$$

The summation convention with respect to repeated indices is being used and a comma before an index denotes differentiation with respect to that spatial coordinate. σ_{ij} are the true symmetric Cauchy stresses. The virtual rate of deformation tensor δd_{ij} is defined by

$$\delta d_{ij} = \frac{1}{2}(\delta v_{i,j} + \delta v_{j,i}) \qquad (2)$$

in which δv_i are components of any compatible field of virtual velocities. T_i are the components of the prescribed surface forces per unit surface. dV and dS_T are volume resp. elements of boundary surface where tractions are prescribed.
The rate of the virtual power equation is derived by taking the material time derivative ($\dot{-}$) of eq. (1), which leads to the following equation

$$\int_V [\dot{\sigma}_{ij} - \sigma_{ik} v_{j,k} + \sigma_{ij} v_{k,k}]\ \delta v_{i,j}\, dV =$$

$$= \int_{S_T} (\dot{T}_i + T_i v_{k,k})\ \delta v_i dS_T \qquad (3)$$

The assumption is made that the material is homogeneous and isotropic and a linear relation between stress rates and strain rates is being adopted. As has been shown

by Nemat-Nasser [4] a linear decomposition of the deformation rate (d_{ij}) into elastic (d^e_{ij}) and plastic parts (d^p_{ij}) is valid

$$d_{ij} = d^e_{ij} + d^p_{ij} \qquad (4)$$

The rate of plastic dilatation (d^p_{kk}) is zero. In the constitutive equations frame independent stress rates and deformation rates have to be chosen. This leads to the following relation between the corotational Jaumann rate of Cauchy stresses $(\dot{\sigma}_{ij})^J$ and the rate of elastic deformations

$$(\dot{\sigma}_{ij})^J = C_{ijkl} d^e_{kl} \qquad (5)$$

C_{ijkl} is the linear elastic material stiffness tensor for isotropic material. The relation between the Jaumann rate and the material derivative of Cauchy stresses is as follows [5]

$$(\dot{\sigma}_{ij})^J = \dot{\sigma}_{ij} + \omega_{ik}\sigma_{kj} - \sigma_{ik}\omega_{kj} \qquad (6)$$

In this equation the tensor ω_{ij} is the rate of rotation tensor being defined by

$$\omega_{ij} = \frac{1}{2}(v_{j,i} - v_{i,j}) \qquad (7)$$

The yield criterion being adopted is the von Mises' criterion for isotropic hardening material. The hardening characteristic of the material has been assumed to be a function of the total plastic work dissipation per unit deformed volume.

At plastic loading the rate of plastic deformation vector has the direction of the outward normal to the yield surface in stress space (normality rule).
Basing upon the assumptions mentioned above, one can now write eq. (5) for plastic loading as

$$(\dot{\sigma}_{ij})^J = (C_{ijkl} - Y_{ijkl})\, d_{kl} \qquad (8)$$

Y_{ijkl} is the plasticity matrix.
To describe kinematic and combined kinematic and isotropic hardening the fraction model approach as proposed by Besseling [6] has been applied. A volume-element of the material is thought to be composed of a conglomerate of subelements (fractions) with differing elastic limits. Kinematic hardening of the material is obtained when all fractions behave elastic-ideally plastic. When one or more fractions have an elastic-isotropic hardening behaviour the material will show a combined kinematic-isotropic hardening effect.
By adjustment of the number of fractions, their yield limits, participation factor and isotropic work hardening the behaviour of materials exposed to fluctuating or cyclic loads can be described.
Substitution of eqs.(6,7) in eq. (8) gives after some manipulation

$$\dot{\sigma}_{ij} = (C_{ijkl} - Y_{ijkl} - C^*_{ijkl})d_{kl} + v_{i,k}\sigma_{kj} + v_{j,k}\sigma_{ik} \qquad (9)$$

with $$C^*_{ijkl} = \frac{1}{2}(\sigma_{jl}\delta_{ik} + \sigma_{jk}\delta_{il} + \sigma_{il}\delta_{jk} + \sigma_{ik}\delta_{jl})$$

The tensors C_{ijkl}, C^*_{ijkl} and Y_{ijkl} are all symmetric in the indices i and j,k and l,ij an kl.
Substitution of eq. (9) in the time derivative of the virtual power equation

(eq.(3)) and neglecting the term $\sigma_{ij}v_{k,kj}$, which is allowable when the stress divided by the elastic modulus is small compared to unity, the following rate of power equation is being derived

$$\int_V [\,(C_{ijkl} - Y_{ijkl} - C^*_{ijkl})d_{kl} + \sigma_{kj}v_{i,k}\,]\,\delta v_{i,j}dV = \int_{S_T} \dot{T}_i \delta v_i dS_T \qquad (10)$$

All variables in this equation are referred to the current configuration.
To solve the governing virtual equation now in an approximate way, the body in its current configuration is discretized in finite elements, which in fact are defined by the spatial coordinates of the nodes of the initially undeformed mesh, the position of these nodes having been updated during the solution process.
The discretization of "time" is being attained by applying incremental steps of prescribed loads and/or displacements, supposing that during these steps the position, geometry and stiffness of the elements do not change and so the structure behaves like a linear one. All variables are related to the state at the beginning of the relevant load step. The increments of nodal displacements having been found by solving the discretized and linearized equations resulting from eq. (10) now naturally do not correspond with these of the actual structure. The geometric non-linearities cause a deviation from reality and by supposing linear behaviour, the stresses in those elements subjected to plastic loading will drift from the yield surface and must be corrected.
To maintain or bring the state of stress in the integration points of the elements on the yield surface at plastic loading, a corrective method much alike the one described by Rice and Tracey [7] has been used. The stress increments are further corrected in an integrative way by dividing the nodal displacement increments in a number (say m) equal subincrements. The stress increments caused by the load step are determined now from a series of subincremental stresses, which are obtained by substituting the subincremental nodal displacements in the incremental constitutive equations.
All variables in the constitutive equations are related to the configuration just before the application of the pertinent displacement subincrement, the coordinates of the nodal points being updated m times for the relevant load increment. As the applied nodal forces now do not match the computed stresses, these forces are corrected by computing - by means of the virtual power equation - a corrective nodal load vector, which is taken account of in the next load step.
The program developed for plane stress, plane strain and axial symmetric problems contains the isoparametric quadrilateral element with a four-point integration rule.
As a consequence of the condition of incompressibility with fully plastic incremental deformations, the number of kinematic constraints for plane strain and axi-symmetric problems limits the actual number of degrees of freedom of the finite element mesh drastically and unrealistic solutions may be obtained. To overcome this difficulty a modified deformation rate as proposed by Nagtegaal et al. [8] has been incorporated in the program.
The program has the possibility to prescribe the behaviour of the elements per element group: linear elastic, elastic-plastic infinitesimal strains, elastic-plastic finite strains.

MATERIAL CHARACTERISTICS

To compute stresses and deformations around the tips of cracks where large deformations occur it is of vital importance to base these computations upon one-dimensional true stress-natural (logarithmic) strain curves which are realistic in the large deformation range. As such a curve for AISI-304 material is not available from literature, experiments have been done in our laboratories with a MTS-testing machine coupled to a PDP-11 processcomputer. These tests comprise tensile tests with four 6 mm-diameter cylindrical specimens, which have been

pulled up to an engineering strain of about 8% at a speed of 0.15%/sec. and with 8 axisymmetric specimens to determine the true stress-natural strain curve up till fracture. These latter specimens which have been pulled at a speed of 0.2%/sec. measured at the neck have been given an initial radius of axial curvature of 50 mm and an initial minimum diameter of 6 mm. The axial curvature promotes the localisation of the neck, enabling in this way a correct measurement of the minimum diameter of the cross section.
From these tests the average value of the stress across the neck, being the load F divided by the current area of the neck A, is plotted in Fig. 1 versus the natural strain (denoted by $\ln(L/L_o)$) measured in the neck of the specimen and which, with A_o being the initial area in the neck equals $\ln(A_o/A)$. In this figure the band of spread of the experimental data is shown by the hatched area.
To describe the hardening character of this material, the results of the cyclic-strain tests which were performed by TNO, Metaalinstituut in The Netherlands on tubular specimens could be gratefully used. The diameter of the cylindrical inner surface of these specimens is 25 mm. The specimens have been given an axial curvature with radius of 300 mm. The minimum wall thickness is 2 mm. The gauge length is 32 mm. A finite element computation has been made of these tubular specimens under cyclic-strain loading and by adjustment of the different parameters contained in the fraction model, a reasonable description could be obtained.

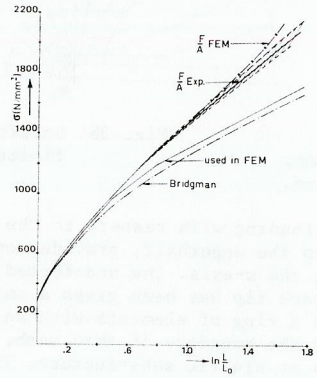

Fig. 1. Stress-natural strain curves.

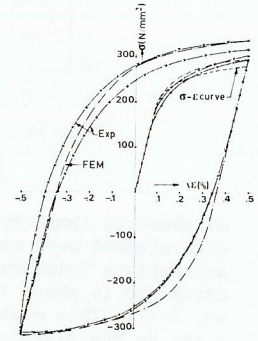

Fig. 2. Experimental and computed 1st cyclic-strain curves for AISI-304. $\Delta\varepsilon = \pm 0.5\%$

In Fig. 2 the experimental cyclic-strain curves for the first cycle for 2 different specimens and the computed curve are shown. In the figure the stress-strain curve, as found by the tests on the 6 mm diam. cylindrical specimens, and upon which curve the above mentioned computations have been based, is also shown.
The material was modelled by taking 4 fractions. One of these fractions has been given a small participation factor but a fair amount of isotropic hardening. The other fractions behave elastic-ideally plastic. All fractions are in the plastic range at a strain of 0.4%. With this material model saturation occurs after about 4 cycles, which is in fair agreement with the experimental results.
After the beginning of necking in the tensile specimens, the stresses as found from the formula F/A must be corrected. With the well known Bridgman formula [9] this corrected curve is shown in Fig. 1 as well. This Bridgman-corrected curve now has been checked by a finite element computation of the same tensile specimen. By comparing the results of this calculation with the experimental results it appeared

that this corrected stress-strain curve underestimates the true stresses. The stress-strain curve which reasonably matches the experimental data is the multilinear curve shown in Fig.1, indicating that the Bridgman correction leads to an underestimation of the stresses of max. 4%. The result of the finite element computation based upon this multilinear curve is shown in Fig. 1 by the curve with crosslets. The behaviour of AISI-304 being adequately modelled in the way described above, has been used in further studies.

NEAR-CRACK TIP FIELDS

The computations of stresses, strains and other relevant quantities near the tip of a crack have been performed for a Compact Tension Specimen (CTS), loaded in the range of small scale yielding. The main dimensions of the CTS are shown in Fig. 3a.

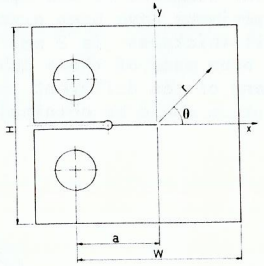

Fig. 3a. Compact Tension Specimen. a= 100 mm, H=240mm, W= 200 mm.

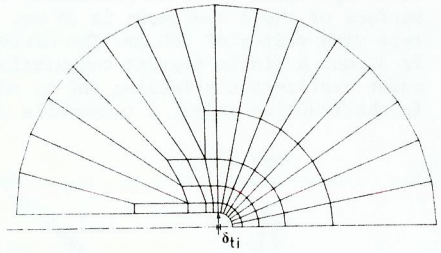

Fig. 3b. Undeformed near tip finite element mesh.

As there is symmetry of geometry and loading with respect to the x-axis, the finite element mesh can be restricted to the upperhalf, provided one prescribes appropriate boundary conditions along the x-axis. The undeformed mesh near the crack tip is shown in Fig. 3b. The crack tip has been given a small initial radius: $\delta_{ti}/2$. This mesh is surrounded by a ring of elements with an outer radius of 5 mm. As the plastic zone lies within the boundary of this mesh, the elements outside this region have been treated as an elastic substructure. The number of quadrilateral elements in the mainnet is 187. The number of degrees of freedom is 426. The computations have been made on a DEC-10 computer at the Twente University of Technology. They have been carried out for elastic-ideally plastic material (el.-id. pl.) and for AISI-304 in plane strain conditions.
The "specimens" have been loaded upto a stress-intensity factor K_I given in Table I. Next the load has been removed and then applied for the 2nd time to its maximum value.

TABLE 1. Different data, defined in text.

	el.-id.pl.	AISI-304
σ_o (N/mm^2)	250	180
E (N/mm^2)	7.5 x 10^4	2 x 10^5
ν	0.3	0.28
max. K_I (N/mm$^{\frac{3}{2}}$)	1560	1250
δ_{ti} (μm)	12.0	4.2
max. δ_t/δ_{ti}	7.4	3.1

The number of incremental steps, applying the load for the first time is approximately 150. In Table I the yield point in uniaxial tension σ_o, the elastic modulus E, Poissons' ratio ν, the max. stress intensity factor K_I, the initial notch width

δ_{ti} and the ratio of computed width δ_t at max. load and δ_{ti}, have been given for both materials.

From the large quantity of data only a small part can be presented in this paper. The size and shape of the plastic zone for el.-id.pl. agree reasonably well with the results found by Larsson and Carlsson [10] with a max. radius of 0.13 (0.11 by L & C)$\times(K_I/\sigma_o)^2$. After load removal the max. radius of the reversed plastic zone for this material is about one third of this value.
In Fig. 4 the deformed geometries of the blunted near tip mesh for both materials at max. load are shown. Attention is being drawn to the hump near the blunted tip in the ideally plastic case.
The Crack Tip Opening Displacement (CTOD) defined by $(\delta_t - \delta_{ti})$ measured at the point shown in Figs. 3 and 4 conform fairly well with results found by McMeeking [2] for el.-id.pl., resulting in the formula

$$CTOD = C(1-\nu^2)\, K_I^2/(E\sigma_o) \qquad (11)$$

with C = 0.65

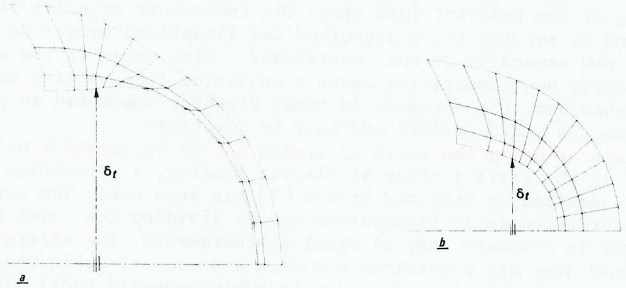

Fig. 4. Near tip deformed meshes
a) elastic-ideally plastic
b) AISI-304

For the hardening AISI-304 the notch width is far less defined as may appear from Fig. 4b. Moreover the constant C in eq. (11) now appears to be a function of load, decreasing (for the position chosen)from about 0.35 at zero to 0.215 at max. load.

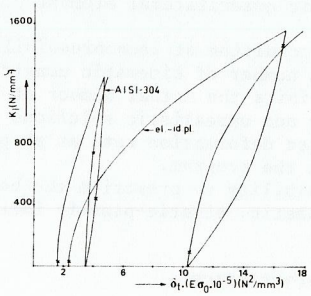

Fig. 5. Crack tip opening δ_t (times $E\sigma_o.10^{-5}$) at cycling load as function of K_I for el.-id.pl. and AISI-304.

In Fig. 5 the notch width δ_t has been plotted as a function of K_I for the whole loading history and for both materials. It shows clearly that after load removal the width is still quite considerable. Crack closure does not occur as the crack does not grow. After applying the load for the 2nd time the notch width is larger

than the first time. In the figure the points where in the first element all fractions become plastic at loading and unloading have been indicated by crosslets. For el.-id.pl. the near tip normal stresses divided by σ_o for points ahead of the crack on the x-axis have been plotted in Fig. 6a as a function of the position of the point relative to the notch surface in the undeformed configuration along the x-axis (R) divided by the notch width δ_t. At the notch surface the stress σ_y agrees with the analytical value of 1.15 σ_o, the stress σ_x being nearly zero there, as it must be. The max. value of σ_y is 3.1 σ_o at R/δ_t = 3.8. As found by McMeeking [2] these stress fields remain unchanged as function of R/δ_t above a load corresponding to appr. K_I = 800 N/mm$^{3/2}$ probably indicating that at this load - when δ_t is about 2.5 times its initial value - the blunted crack tip has obtained its ultimate shape. Fig. 6a also shows the results found by McMeeking [2] and Rice and Johnson [1].

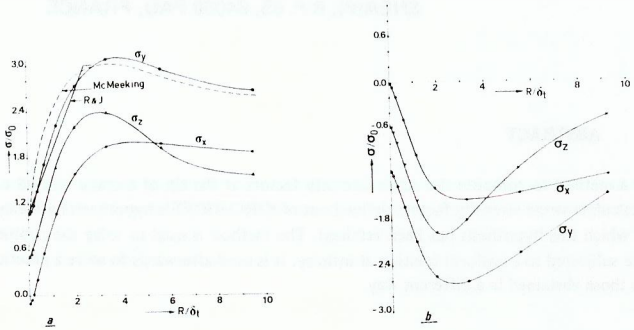

Fig. 6. Near tip stress distributions for el.-id.pl. ahead of crack tip.
a) above K_I = 800 N/mm$^{3/2}$. With results of McMeeking and Rice and Johnson
b) after load reversal at zero load.

In Fig. 6b the residual stresses near the tip remaining after load removal have been plotted for the same points as a function of R/δ_t. The max. value of the compressive stress σ_y is 2.7 σ_o at R/δ_t = 2.7. After the application of the load the 2nd time the same stresses are found as the first time. The stress σ_z equals $(\sigma_x + \sigma_y)/2$ in the region R/δ_t<2, indicating that the material behaves fully plastic in that region.

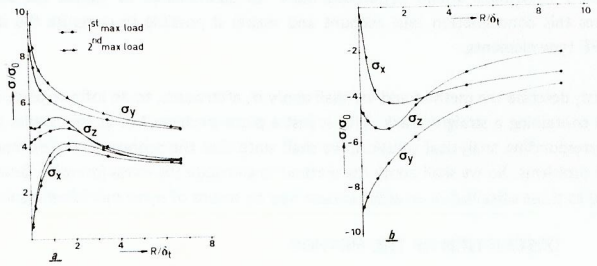

Fig. 7. Near tip stress distributions for AISI-304 ahead of crack tip
a) at max. loads, 1st and 2nd time
b) after load reversal at zero load.

For AISI-304 the near tip normal stresses, divided by σ_o for points ahead of the crack have been plotted in Fig. 7a as a function of R/δ_t at first and 2nd max. load.

Clearly the stresses after applying the load the 2nd time now do not equal those occuring the first time. Attention is being drawn to the sharp increase of stresses close to the notch surface, arising from the elevation of flow stress by the large plastic strains in that area. The stresses after load reversal at zero load are plotted in Fig. 7b.

In the next two figures the extensional strain being the total extension of a line element divided by its original length is plotted for elements in x- and y- directions through points on the x-axis ahead of the crack. These strains E_x and E_y for 1st and 2nd max. load resp. after load reversal at zero load, are plotted for el.-id. pl. in Fig. 8 and for AISI-304 in Fig. 9.

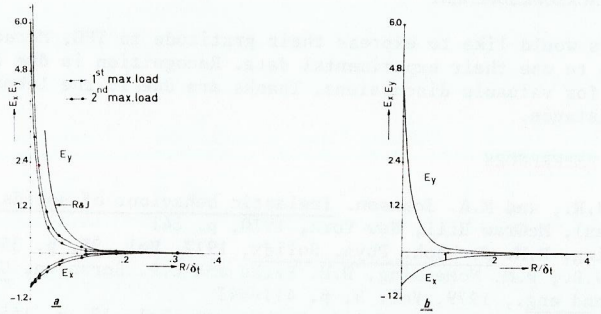

Fig. 8. Extensional strains E_x and E_y ahead of crack tip for el.-id.pl. mat.
a) at max. loads 1st and 2nd time Results of Rice and Johnson
b) after load reversal at zero load

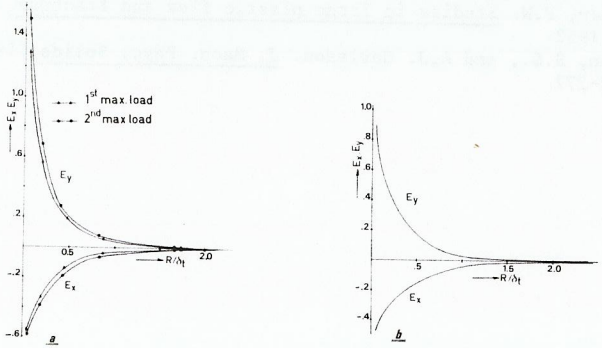

Fig. 9. Extensional strains E_x and E_y ahead of crack tip for AISI-304
a) at max. loads 1st and 2nd time
b) after load reversal at zero load.

In the intense strain zone the strain E_y increases sharply towards the notch surface. After applying the load for the 2nd time this strain is larger yet than the first time. As the extensional tangential strain at the notch surface is proportional to the value $(\delta_t - \delta_{ti})/\delta_{ti}$, this agrees with the result that the notch width after the 2nd load application is larger than the first time. The strain E_x approximates the value -1 near the notch surface for el.-id.pl., which is in agreement with the vanishingly small width of the elements, directly at the blunted crack tip (see Fig. 4a).
The finite shear deformation being defined by the change of the angle of $\pi/2$ between undeformed line elements in x- and y- directions, has a maximum at the notch surface of 1.5 rad. and 1.1 rad. for resp. el.-id.pl. and AISI-304 both in a region θ = 0.6 - 1.2 rad. The maximum computed rotations for elements at the notch surface is about 0.26 rad. for both materials.

ACKNOWLEDGEMENT

The authors would like to express their gratitude to TNO, Metaalinstituut, for the permission to use their experimental data. Recognition is due to prof. dr. ir. P. Meyers for valuable discussions. Thanks are due to the laboratory staff for their assistance.

REFERENCES

1. Rice, J.R., and M.A. Johnson. Inelastic behaviour of solids (ed. by M.F. Kanninen), McGraw Hill, New York, 1970, p. 641
2. McMeeking, R.M. J. Mech. Phys. Solids, 1977, Vol. 25, p. 357-381
3. Rice, J.R., R.M. McMeeking, D.M. Parks and E.P. Sorensen. Comp. meth. in appl. mech. and eng., 1979, Vol. 9, p. 411-442
4. Nemat-Nasser, S. Int. J. Solids Structures, Vol. 15, p. 155-166
5. Fung, Y.C. Foundations of solid mechanics, Prentice Hall, 1965
6. Besseling, J.F. Jrnl. Appl. Mech., Dec. 1958, p. 529-536
7. Rice, J.R. and D.M. Tracey. Computational fracture mechanics in numerical and computer methods in structural mechanics (ed. by S.J. Fenves and others), Ac. Press, New York, 1973, p. 585
8. Nagtegaal, J.C., D.M. Parks and J.R. Rice. Comp. meth. in appl. mech. and eng., 1974, Vol. 4, p. 153-177
9. Bridgman, P.W. Studies in large plastic flow and fracture, McGraw Hill, New York, 1952
10. Larsson, S.G., and A.J. Carlsson. J. Mech. Phys. Solids, 1973, Vol. 21, p. 263-277